

NASA Contractor Report 178248

The Effect of Heavy Rain on an Airfoil at High Lift

Collection of papers presented at the 23rd Annual Meeting of the American Society of Mechanical Engineers, Vol. 1, pp. 1-10, 1987.

Coleman duP. Donaldson and Roger D. Sullivan

*ARAP Group, Titan Systems, Inc.
Princeton, New Jersey*

Contract NAS1-18088

March 1987

NASA

National Aeronautics and
Space Administration

Langley Research Center
Hampton, Virginia 23665-5225

NASA Contractor Report 178248

The Effect of
Heavy Rain on an
Airfoil at High Lift

Coleman duP. Donaldson and Roger D. Sullivan

*ARAP Group, Titan Systems, Inc.
Princeton, New Jersey*

Contract NAS1-18088

March 1987

NASA

National Aeronautics and
Space Administration

Langley Research Center
Hampton, Virginia 23665-5225

1. Introduction

Although the effect of heavy rain on aircraft performance was discussed as early as 1941 by Rhode (1), no serious studies of the relationship of heavy rain to aircraft safety were made until Luers suggested in 1981 that the torrential rain that often occurs at the time of severe wind shear might substantially increase the danger to aircraft operating at slow speeds and high lift in the vicinity of airports. While Luer's ideas were not published until early 1983 (2), appropriate measures were taken by NASA to study the effect of heavy rain on the lift of wings typical of commercial aircraft. These tests, reported by Dunham, Bezos, Gentry, and Melson (3), were the subject of a number of discussions between the senior author of this report and Mr. Earl Dunham of NASA during the fall of 1984. One of the aspects of these tests that seemed confirmed by the data was the existence of a "velocity effect" on the lift data. The data seemed to indicate that when all the normal non-dimensional aerodynamic parameters were used to sort out the data, the effect of velocity was not accounted for, as it usually is, by the effect of dynamic pressure. Indeed, the measured lift coefficients at high lift indicated a drop-off in lift coefficient for the same free-stream water content as velocity was increased.

This behavior was explained at the time by the authors as being due to the variations in momentum deposition of the droplets that are splashed back into the air stream after shattering upon striking the airfoil surface. Since the higher the speed the smaller are the splashed back droplets, it follows that the higher the speed the closer to the airfoil will be the layer where these droplets are reaccelerated by the air stream. It was suggested that if this splashed-back momentum effect was large enough and took place close enough to the airfoil, the airfoil could stall. This would be a very serious condition if, indeed, it could occur. These ideas were put forward at a meeting of contractors working the heavy rain problem for NASA in April of 1985 (4).

Subsequent to this meeting, funds were obtained from NASA to modify the A.R.A.P. ARB code to allow the computation of the effect of splashed back droplets on the location of separation on airfoils at high angle of attack to see if stall could be induced and under what conditions of speed and scale such a phenomenon might be hazardous to aircraft operation. A secondary objective of this calculation was to obtain such information as could be gleaned to aid NASA in conducting properly scaled tests of airfoils in heavy rain.

Bilanin (5) has given a more detailed review than is attempted here of the mechanisms that may be involved when aircraft operate in heavy rain.

2. Ejecta Scaling

To derive an expression for the extent of the momentum-defect layer that results from droplet splash-back, we first determine the order of magnitude of the diameter of the droplets that splash back from a surface after drop impingement.

We consider a drop of radius r_0 impinging normally with velocity V on a frictionless surface unwetted by the drop. As the drop hits the surface it is deformed into a pancake whose instantaneous radius is a and whose thickness is t as shown in Figure 2.1. From continuity, we have the result that

$$\frac{4}{3} \pi r_0^3 = \pi a^2 t \quad (1)$$

At any given time, the surface energy of the distorted pancake is

$$\sigma_w (2\pi a^2 + 2\pi a t) \quad (2)$$

where σ_w is the surface tension of water in contact with air.

In view of (1), this may be written

$$\frac{4}{3} \pi r_0^3 \left(\frac{2}{t} + \frac{2}{a} \right) \sigma_w \quad (3)$$

Generally when the drop breaks up into droplets, $t \ll a$, so we write the surface energy approximately as

$$\frac{4}{3} \pi r_0^3 \cdot \frac{2}{t} \sigma_w \quad (4)$$

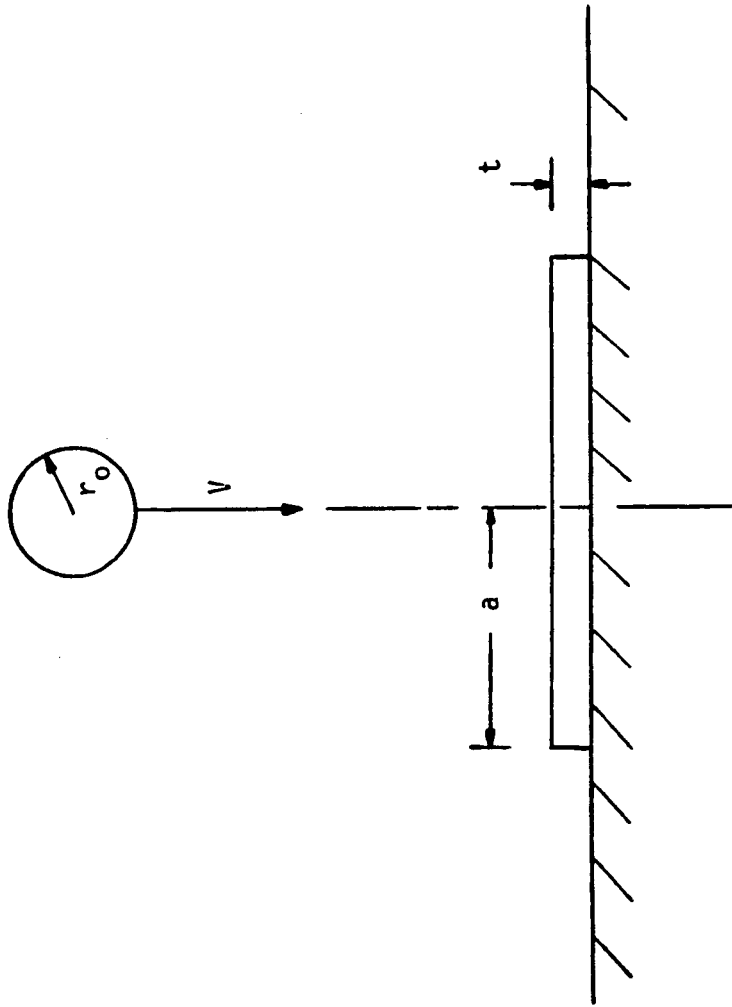


Figure 2.1 Geometry of drop impingement.

Now this surface energy cannot increase without bound as t becomes smaller, for the only energy available to supply this surface energy is the kinetic energy of the original drop. In an actual impingement process, energy is lost to both internal and external friction, but if we neglect these and other losses and say that droplets of diameter $d_p = t$ must form where a portion of f of the original kinetic energy has been converted to surface energy, we may write

$$f \frac{\rho_w V^2}{2} \cdot \frac{4}{3} \pi r_0^3 = \frac{4}{3} \pi r_0^3 \frac{2\sigma_w}{t} \quad (5)$$

or

$$d_p = t = \frac{4}{f} \frac{\sigma_w}{\rho_w V^2} \quad (6)$$

The above expression gives the order of magnitude of droplet size that can be formed. From this expression we learn that the faster one flies through the air the smaller are the drops that are splashed back from the surface of an airfoil. Also, we see that the droplet splash-back size is expected to be relatively independent of the initial drop size r_0 .

Having obtained an expression for the size drop one expects to see splashed back, we may now derive an expression for a length that is typical of the distance over which the splashed drops are accelerated. Consider the deceleration of a particle by its drag:

$$m_p \frac{dV}{dt} = C_D \frac{\rho_a V^2}{2} A_p \quad (7)$$

where m_p and A_p are the mass and cross-sectional area of the particle, C_D is the coefficient of drag, ρ_a is the air density, V is the magnitude of the velocity, and t is time. We may write this, since $ds = Vdt$, as

$$\frac{dV}{V} = - \frac{C_D A}{m_p} \cdot \frac{\rho_a}{2} ds \quad (8)$$

There is clearly a characteristic length associated with the acceleration process, and if we assume $C_D \cong 1$ it is

$$l_c = \frac{m_p}{A_p} \cdot \frac{2}{\rho_a} \quad (9)$$

What Eq. (9) tells us is that droplets splashed back from the surface of an airfoil will have the momentum defect that they bring into the air flow about the airfoil adjusted within a distance of the order of l_c from the surface. We may look at this length then as a momentum-defect deposition or adjustment length. We may express this length in terms of the splash droplet diameter, d_p , by noting that for a sphere

$$\frac{m_p}{A_p} = \frac{2}{3} \rho_w d_p \quad (10)$$

where ρ_w is the density of water. Putting Eq. (10) into Eq. (9) we obtain

$$l_c = \frac{4}{3} \frac{\rho_w}{\rho_a} d_p \quad (11)$$

Using the diameter d_p given in (6) we find finally that the momentum-defect adjustment length is

$$\ell_c = \frac{16}{3f} \frac{\sigma_w}{\rho_a V^2} \quad (12)$$

What will be important in considering the effect of the momentum defect splashed back by the impinging droplets will be the ratio of this length to a typical dimension of the wing or airfoil in question. We therefore expect that an appropriate parameter for scaling the effect of heavy rain will be

$$\frac{c}{\ell_c} = \frac{3f}{16} \frac{\rho_a V^2 c}{\sigma_w} \quad (13)$$

where c is the chord of the airfoil. We can get rid of the constant $3f/16$ and take as a parameter simply

$$N_D = \frac{\rho_a V^2 c}{\sigma_w} \quad (14)$$

This parameter (the deposition length parameter) is a mixed Weber number containing the density of air and the surface tension of water.

It is useful in order to understand the relative importance of rainfall rate and N_D on $C_{L_{\max}}$, to consider the sketches in Figure 2.2a and 2.2b. In Figure 2.2a we show for a fixed N_D (thus a fixed momentum-adjustment length) an extremely simplified picture of what increasing rainfall rates will do to the velocity distribution on the upper surface of an airfoil at angle of attack. Clearly as the rainfall rate is increased, a larger momentum-defect will be realized, and with increasing defect will come less and less ability of the boundary layer on the upper surface to recover pressure. Thus, we

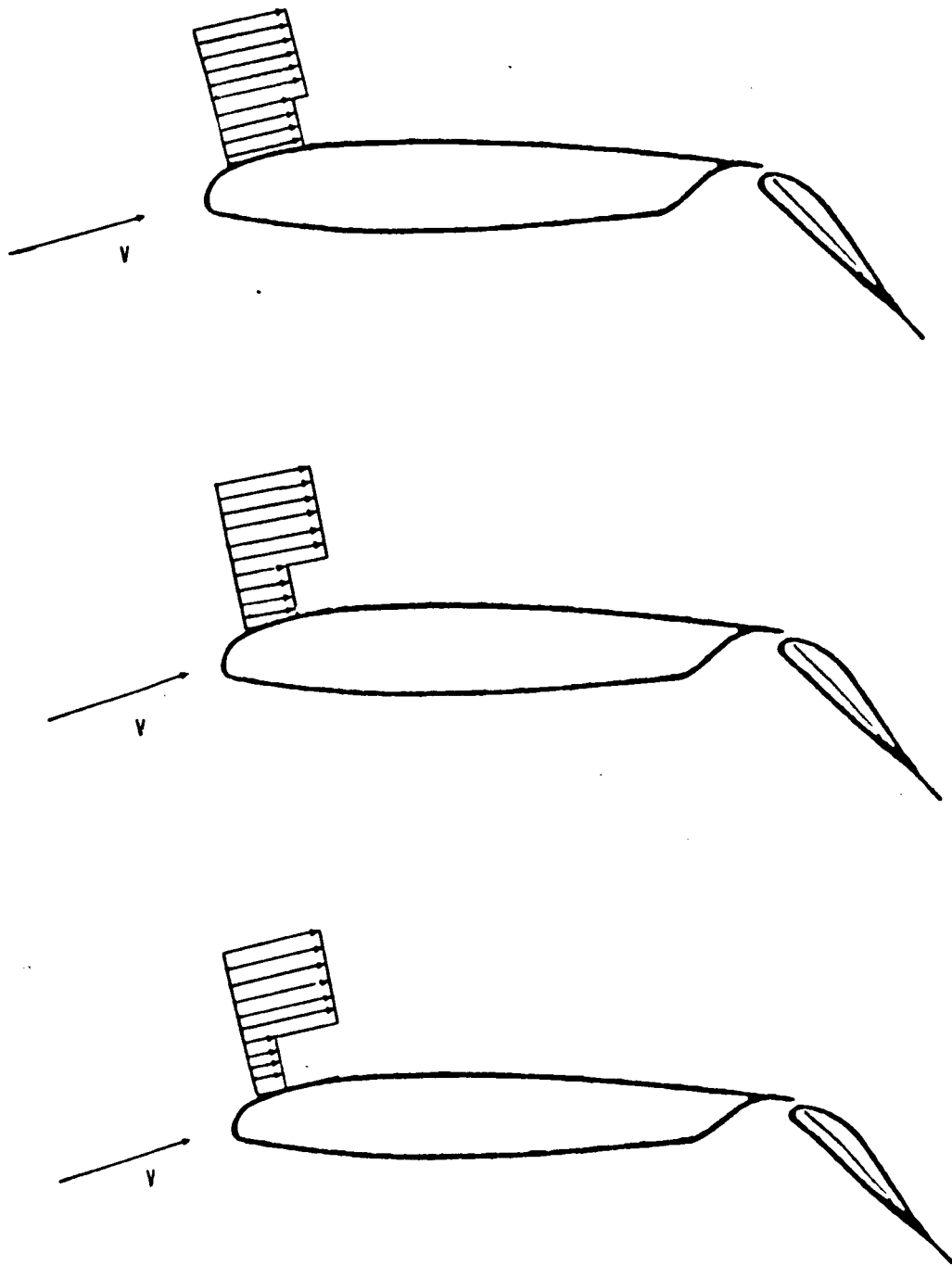


Figure 2.2a Effect of increasing rainfall rate on near-surface velocity distribution at a fixed value of N_D , i.e. fixed momentum-defect adjustment length relative to chord.

might expect the $C_{L_{\max}}$ of an airfoil to fall off (perhaps linearly) as rainfall rate is increased at a fixed value of N_D .

On the other hand, if we consider what happens for a fixed rainfall rate as N_D is increased, we must see something like what is depicted in Figure 2.2b. In this case, as N_D is increased, the momentum adjustment length becomes smaller and smaller; thus a given momentum deficit that is associated with the rainfall rate must be carried in a thinner and thinner layer. The result, at least as far as the flow at the surface is concerned, is equivalent to increasing the rainfall rate. We would expect to find then that the effect of increasing the chord of an airfoil at a fixed rainfall rate might be similar to the effect of increasing rainfall rate for a fixed chord.

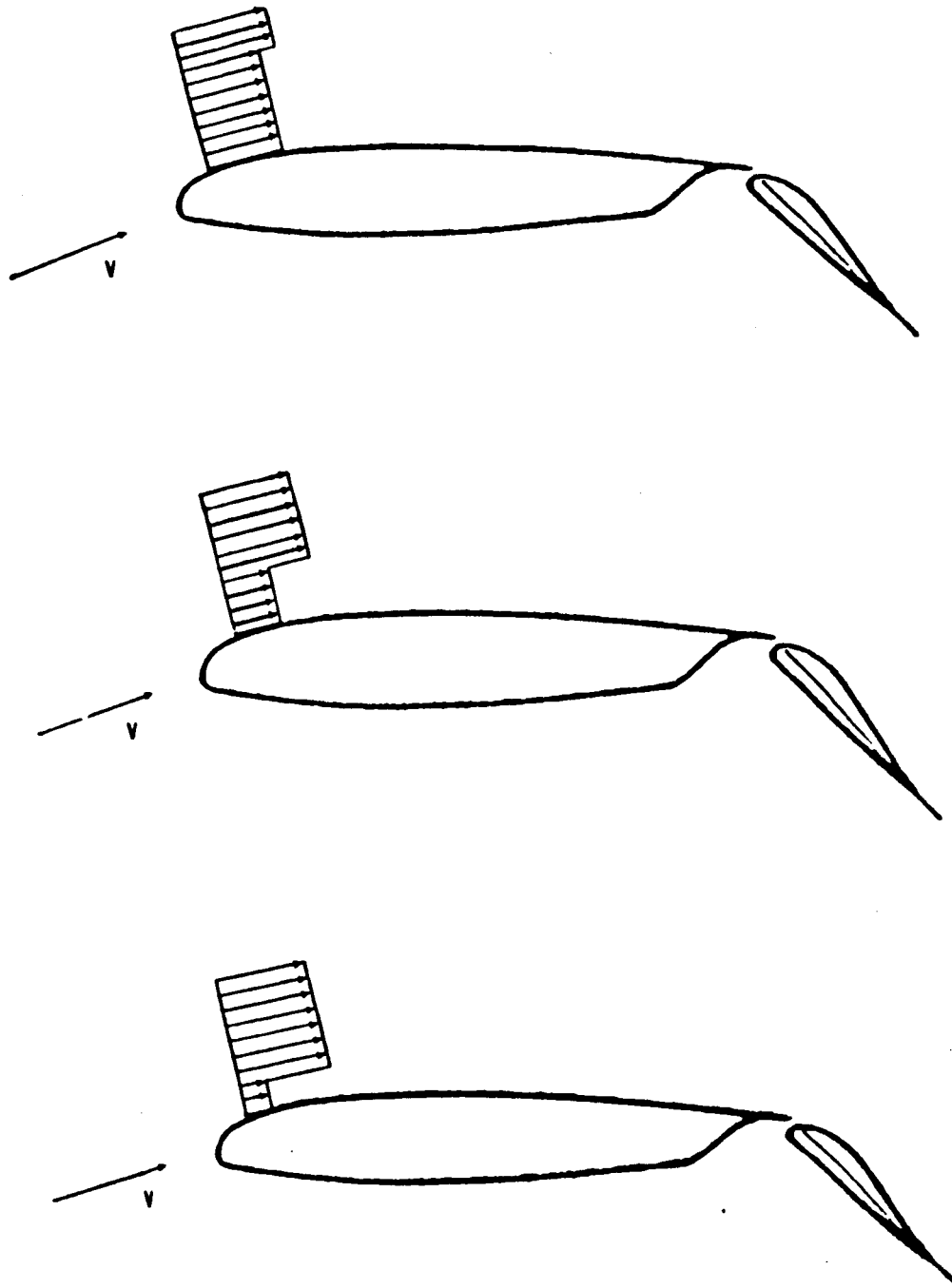


Figure 2.2b Effect of increasing N_D on near-surface velocity distribution at fixed rainfall rate.

3. Initial Examination of Data

A small amount of data on $C_{L_{max}}$ as a function of rainfall rate and N_D was given to the authors by Mr. Earl Dunham of NASA/Langley. These data are shown in Figure 3.1. A fair amount of liberty has been taken in fairing curves through the data on the basis of our feeling that the effect of rainfall rate on $C_{L_{max}}$ might be linear. The fairing was also biased by our notion that the effects of N_D and rainfall rate might be similar.

With great trepidation the results of the initial fairing of these data are shown in Figure 3.2, as a function of N_D with rainfall rate as a parameter. The $C_{L_{max}}$ data are plotted in terms of $1 - C_{L_{max}} / (C_{L_{max}})_0$, where $(C_{L_{max}})_0$ is the value of $C_{L_{max}}$ for zero rainfall rate.

On this figure we have also indicated the range of N_D that will be found for large jet transport aircraft during landing operations and the range of N_D for which water impingement tests have been carried out at MIT.

First of all, it should be noted that Reynolds number is a parameter that must be considered, perhaps by a consideration of the ratio of ℓ_c to the boundary layer thickness. However, it is now believed best to use N_D as given here as the essential parameter and consider Reynolds number effects separately.

In view of the possibility that N_D effects are similar to rainfall rate effects as pointed out above, an initial conjectural extrapolation of the data to the N_D values that might be associated with large scale transports was made and is given in Figure 3.2 for a rainfall rate of 75 mm/hr (3 in/hr). This extrapolation indicated that such a rate might cause a 15 to 20 percent reduction of $C_{L_{max}}$. Clearly the implication of this hypothetical scaling poses a

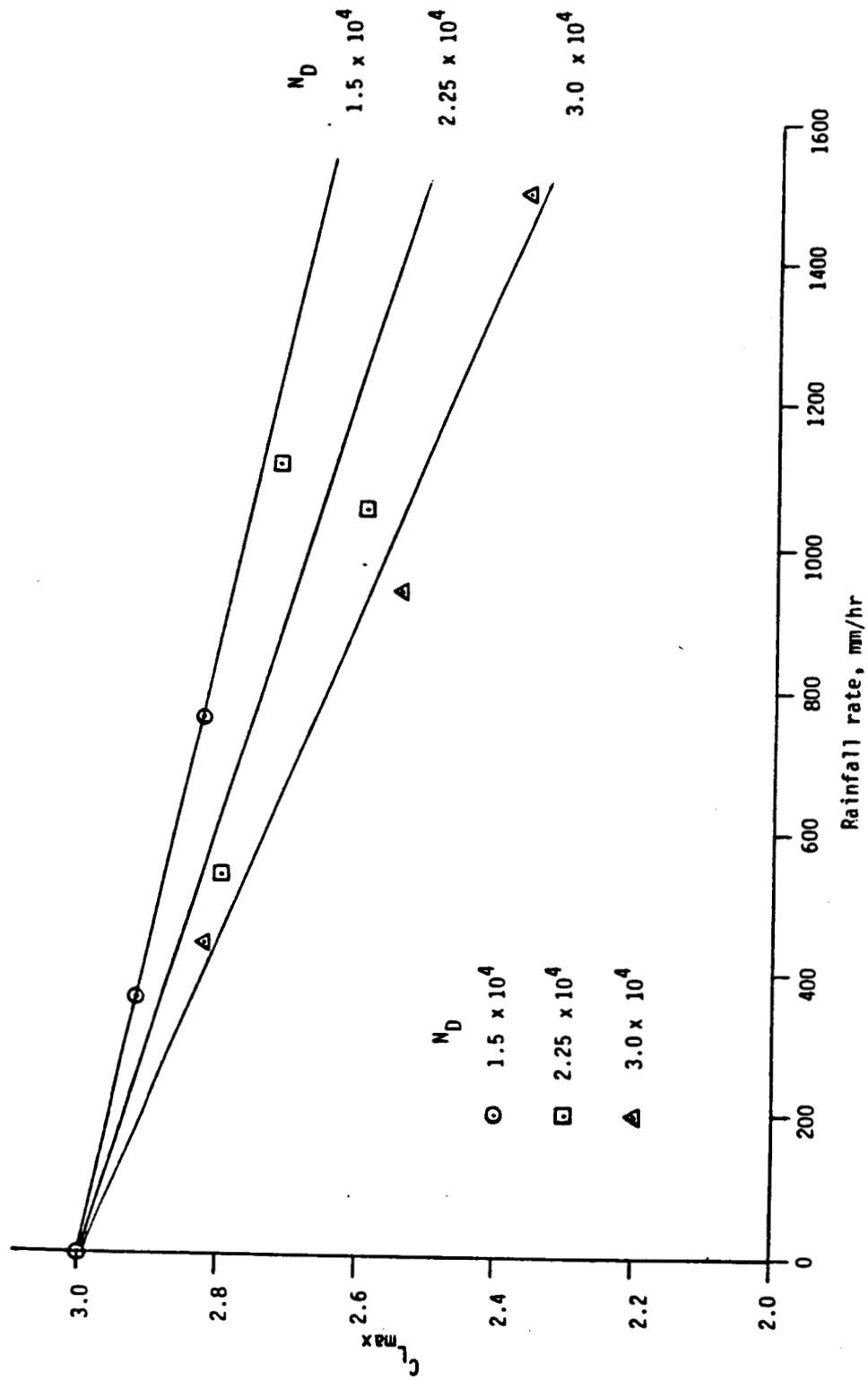


Figure 3.1 NASA data on $C_{L_{max}}$ as a function of rainfall rate with N_D as a parameter.

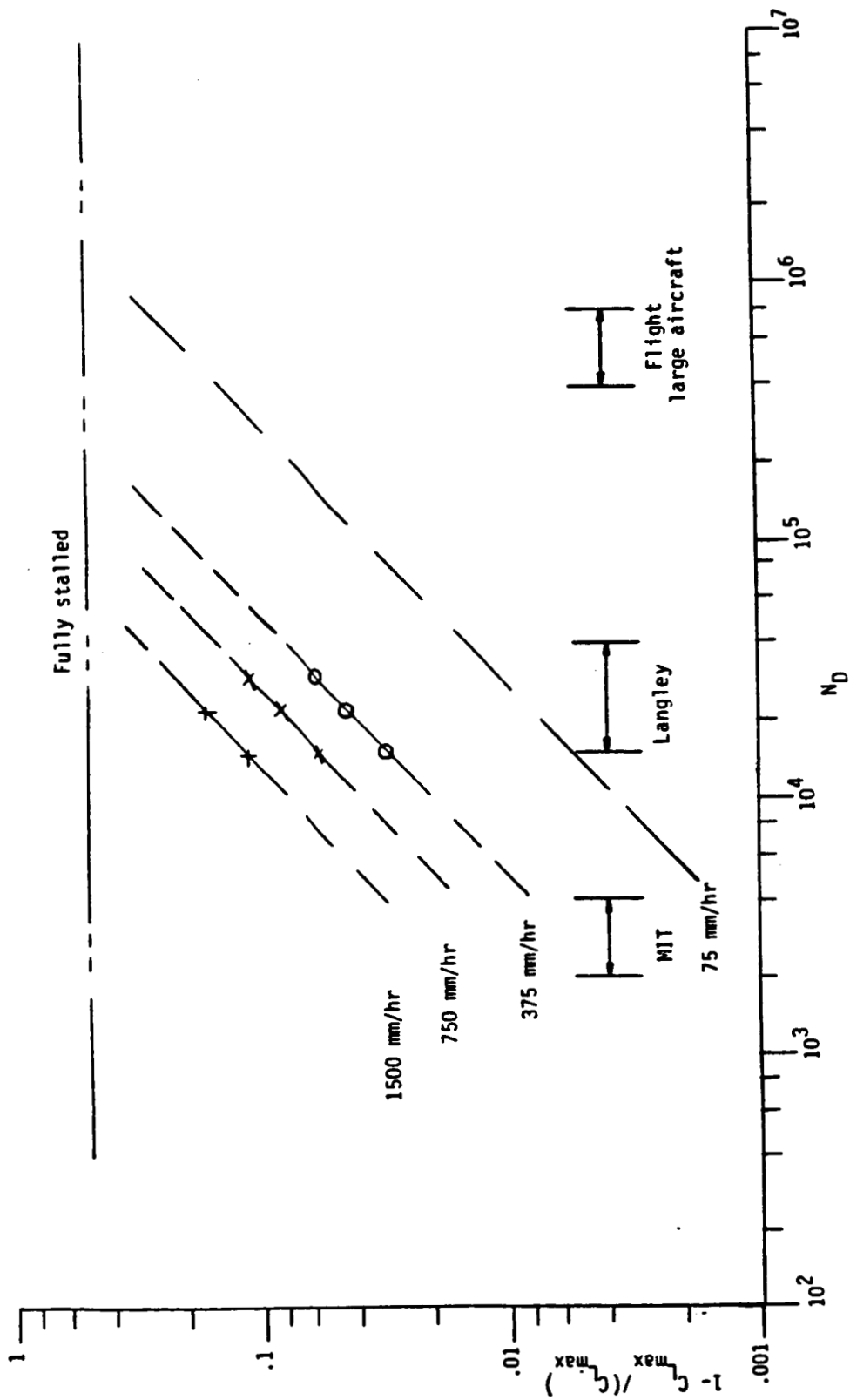


Figure 3.2 Conjectural plotting of NASA data on $C_{L_{max}}$ as a function of N_D with rainfall rate as a parameter.

sufficiently severe operational problem so that a large scale wing should be tested in a rain environment.

In addition it was clear than an attempt to calculate the effect of droplet splash-back on the maximum lift of an airfoil would be a most useful exercise. In what follows we will describe the program that was used to make such calculations and the results of these calculations.

4. Program Development and Use

The calculation of the maximum lift of a two-dimensional airfoil even without rain is not yet a science. Therefore, rather than try to calculate the effect of rain on maximum lift, the effect on the position of separation for an airfoil near maximum lift was studied. An NACA 64-210 airfoil at an angle of attack, α , of 12° was chosen.

To determine the point of separation, a program called ARB, which has been in use at A.R.A.P. for several years (6), was used. ARB, which employs full second-order closure models for turbulence, computes the boundary layer (using standard boundary-layer assumptions) on an axisymmetric body of arbitrary shape, whether rotating or not, as well as on two-dimensional bodies. It handles compressible flows, solving for the extra second-order correlations that exist because of fluctuations in temperature and density, as well as constant-density flows. Since the present study concerns low-speed flows, the constant density mode was used.

A special version of ARB was developed for this project in order to calculate the effect of particles (water droplets) as they splatter back into the boundary layer after hitting the surface of an airfoil. A description of the analysis underlying the modification of ARB follows.

4.1 Motion of a particle in a boundary layer

In analyzing the motion of a particle in a boundary layer, it is assumed that the variation of the mean flow with x , the streamwise direction, is negligible. It is also assumed that the flow is two dimensional and that the effect of particle motion in the third dimension can be neglected after averaging over a large number of particles.

Consider then a particle moving with velocity $\vec{v}_p = (u_p, v_p)$ in a mean flow $\vec{v} = (u, v)$ (functions of y only). In terms of the relative velocity, $\vec{v}_r = \vec{v} - \vec{v}_p$, the force on the particle is

$$\frac{1}{2} C_D A_p \rho_a |\vec{v}_r| \vec{v}_r$$

where C_D is the drag coefficient, A_p is the cross-sectional area of the particle, and ρ_a is the density of air. Then the acceleration of the particle is

$$\frac{d\vec{v}_p}{dt} = \frac{C_D A_p \rho_a}{2m_p} |\vec{v}_r| \vec{v}_r = \frac{C_D}{\ell_c} |\vec{v}_r| \vec{v}_r$$

where m_p is the mass of the particle and

$$\ell_c = \frac{2m_p}{A_p \rho_a}$$

To evaluate the drag coefficient, the particle is assumed to be a sphere of diameter d_p . In terms of the Reynolds number

$$R_p = \frac{|\vec{v}_r| d_p}{\nu}$$

where ν is the kinematic viscosity of air, C_D may be approximated by

$$C_D = \frac{24}{R_p} + 1$$

(See Figure 1.5 in (7).) For a sphere,

$$\ell_c = \frac{4}{3} \frac{\rho_w}{\rho_a} d_p$$

where ρ_w is the density of water, and so

$$C_D = \frac{32\nu}{|\vec{v}_r| \ell_c} \frac{\rho_w}{\rho_a} + 1$$

The acceleration can be rewritten

$$\frac{du_p}{dt} = D_K(u-u_p)$$

$$\frac{dv_p}{dt} = D_K(v-v_p)$$

where

$$D_K = \frac{C_D}{\ell_c} |\vec{v}_r| = \frac{C_D}{\ell_c} \left[(u-u_p)^2 + (v-v_p)^2 \right]^{1/2}$$

In order to evaluate the effect of the particles on the air flow it is necessary to know \vec{v}_p as a function of y . Since

$$v_p = \frac{dy}{dt}$$

the acceleration equations can be written

$$\frac{du_p}{dy} = \frac{D_K}{v_p} (u-u_p)$$

$$\frac{dv_p}{dy} = \frac{D_K}{v_p} (v-v_p)$$

Thus if the initial values of u_p and v_p as a particle comes off the surface are known, and if the flow conditions are known as a function of y , these equations can be integrated and the force evaluated.

If there are n_p particles per unit volume so that the liquid water content is $\rho_p = n_p w_p$, the x component of the total force exerted by the particles on the air, equal and opposite to the drag of the particles, is

$$\rho_p D_p K (u_p - u)$$

per unit volume. This term was added on the right side of the mean momentum equation (x component) in ARB. No way was found to incorporate the effect of the vertical component of the force from the particles on the fluid in the context of the boundary-layer assumptions on which ARB is based, since these assumptions imply that the vertical component of the mean momentum equation is automatically in balance and the vertical component of velocity is computed from the continuity equation.

However it was recognized that if l_c is very small, a particle will give up its momentum to the air almost immediately so that the effect can be simulated by applying a blowing boundary condition with the velocity at the wall, v_w , given by

$$\rho_a v_w = \rho_p v_p(0)$$

The results of these runs are shown in Section 5 as limits for l_{cm}/c equal zero although they were actually run with l_{cm}/c of the order of 2×10^{-5} .

The rate at which the wake of a particle receives energy is

$$-\frac{d}{dt} \left(m_p \frac{|\vec{v}_r|^2}{2} \right) = -m_p \vec{v}_r \cdot \frac{d\vec{v}_r}{dt} = \frac{C_D m_p}{\ell_c} |\vec{v}_r|^3$$

Therefore the rate at which the fluid receives energy per unit volume is

$$\rho_p D_K |\vec{v}_r|^2$$

It is assumed that a fraction, e , of this energy produces turbulence, the rest going into heat. Therefore a source term equal to

$$\frac{e}{3} \rho_p D_K |\vec{v}_r|^2$$

was included in the equations for $\overline{u'u'}$, $\overline{v'v'}$, and $\overline{w'w'}$ which together constitute the turbulent energy. For all the runs described in Section 5, e was taken to be 1/2.

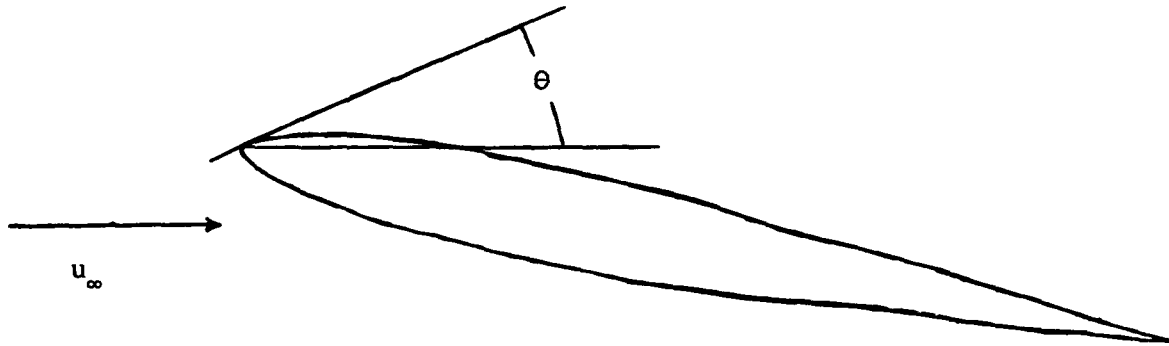
4.2 The variation with streamwise distance

The analysis above assumes that the variation with x is negligible; however as the boundary-layer calculation moves downstream from the stagnation point the flow velocity $\vec{v}(y)$ changes (partly as a result of the force calculated above) and the characteristics of the particles splashed back also change.

Let v_o be the normal component of the velocity of a raindrop as it impinges on the airfoil surface. Then, neglecting the settling speed of the raindrops in comparison with the aircraft speed, u_∞ ,

$$v_o = u_\infty \sin \theta$$

where θ is the local angle of the airfoil surface.



The particles are assumed to leave the surface normally at a given proportion of v_0 , say p . Then

$$u_p(0) = 0$$

$$v_p(0) = pv_0 = pu_\infty \sin\theta = v_{pm} \sin\theta$$

where $v_{pm} = pu_\infty$. It is assumed that no particles are splashed back where θ is zero or negative.

It is shown in Section 2 that l_c is inversely proportional to the square of v_0 so it can be written

$$l_c = l_{cm} / \sin^2\theta$$

where l_{cm} is the minimum value of l_c .

4.3 Pressure distribution

ARB requires the free-stream pressure distribution or the free-stream velocity distribution (from which the pressure distribution can be calculated) as input. For the runs reported in the next section the inviscid flow over the airfoil was calculated by the method developed by J. L. Hess. The results of these calculations were found to be a little noisy so they were passed through a smoother before being supplied to ARB as outer boundary conditions.

The distribution of u_e , the free-stream velocity, as a function of x , measured along the surface from the stagnation point, is shown in Figure 4.1. Figure 4.2 is a diagram of the airfoil at $\alpha = 12^\circ$ with the stagnation point, the leading edge (defined here as the point where $\theta = 90^\circ$), the point of minimum pressure (maximum u_e), and the point of zero slope ($\theta = 0$) indicated. It will be noted that the point of minimum pressure is almost at the leading edge and that on the upper surface a region of large adverse pressure gradient occurs between the leading edge and the point of zero slope. In this region we might expect a very heavy rain to cause the flow to separate and hence cause premature stall of the airfoil.

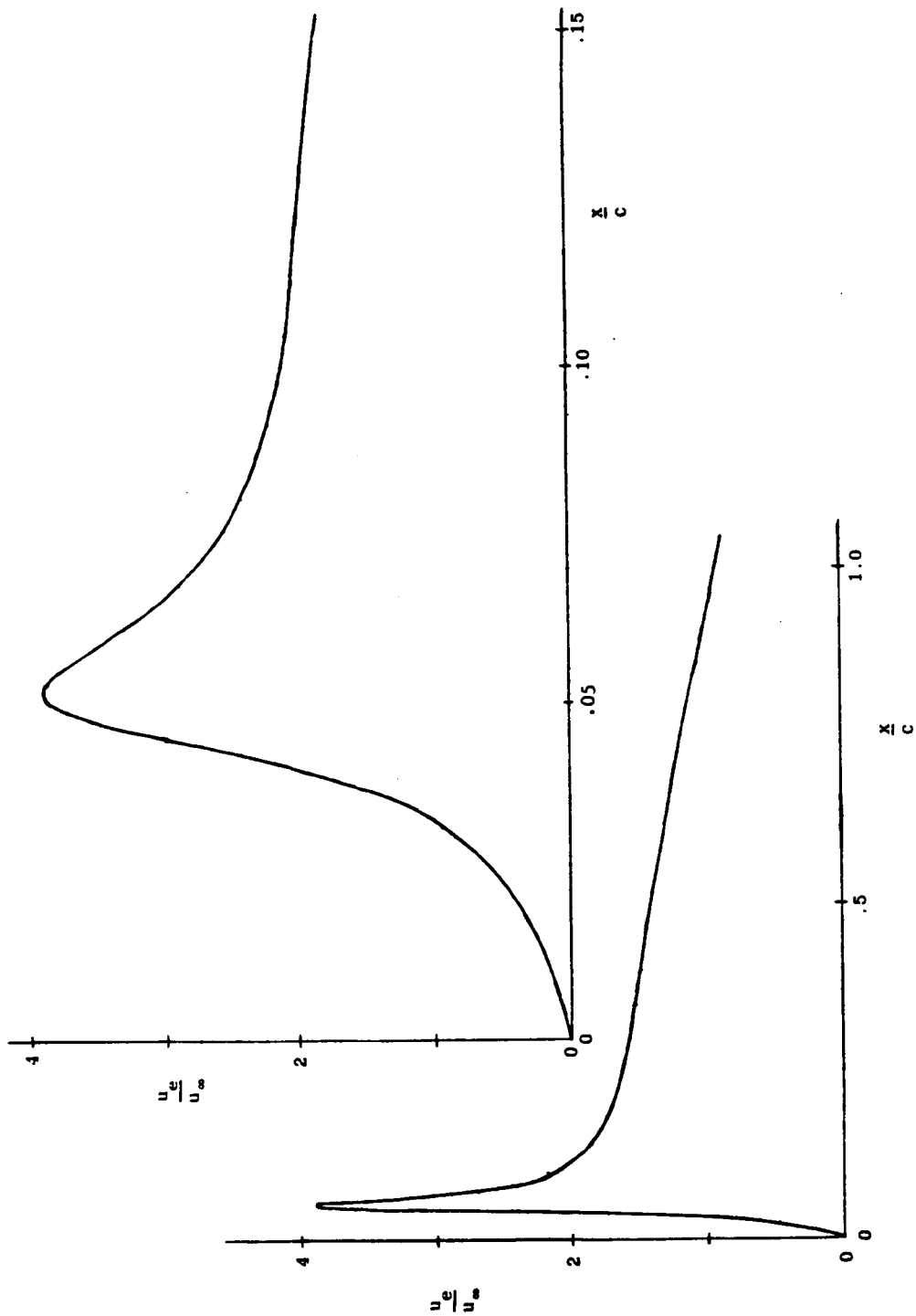


Figure 4.1 Distribution of velocity on the upper surface of an NACA 64-210 airfoil at $\alpha = 12^\circ$ as a function of distance from the stagnation point for inviscid flow.

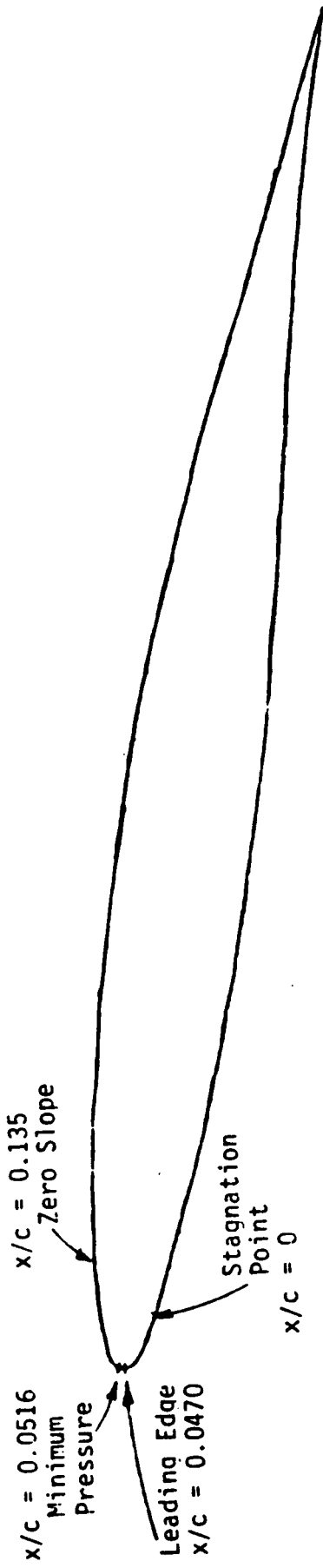


Figure 4.2 Location of critical points on an NACA 64-210 airfoil at $\alpha = 12^\circ$.

5. Computations and Results

Many calculations were made of the behavior of the boundary layer for a number of conditions of rainfall rate (represented by ρ_p), particle size (represented by ℓ_{cm}), initial particle velocity (represented by v_{pm}), and Reynolds number. Figure 5.1 shows typical behaviors of calculated skin friction coefficient, c_f , for three values of ρ_p/ρ_a with $\ell_{cm}/c = 0.001$, $v_{pm}/u_\infty = 0.4$, and a Reynolds number of 3.5×10^7 . This is a Reynolds number typical of a 747 aircraft near landing speed. The curve for $\rho_p/\rho_a = 0$ shows that, as expected, the aircraft does not stall and the point of separation ($c_f = 0$) is near the trailing edge of the airfoil. The curve for $\rho_p/\rho_a = 0.1$, representing a high rainfall rate, shows that the separation point has moved forward somewhat so we might expect some drop-off in C_L but the airfoil has by no means stalled. Note however that the dip in c_f in the region of strong adverse pressure gradient has become more pronounced. The third curve, for a still higher rate, $\rho_p/\rho_a = 0.12$, shows that the separation point has jumped forward to that region and we would expect that the airfoil has stalled.

Figure 5.2 shows the value of x/c at which separation occurs (plotted horizontally) as a function of ρ_p/ρ_a (plotted vertically) for the three runs shown in Figure 5.1 and other runs all at the same ℓ_{cm}/c , v_{pm}/u_∞ , and Reynolds number. It is clear from this figure that the critical value of ρ_p/ρ_a , that required to cause early separation (which we assume is equivalent to stall), is 0.113.

Repeating the process described above for different values of ℓ_{cm}/c , still at the same initial velocity and Reynolds number, we obtain the results shown in Figure 5.3. The open circles are the calculated values of ρ_p/ρ_a required to trigger early separation at various values of ℓ_{cm}/c . When results such as these were first encountered they caused some consternation, for certainly we did not expect the rainfall rate required for early separation to increase as the momentum defect adjustment length, ℓ_c , decreases. The questionable points are connected by a dashed curve in the figure. An analysis of

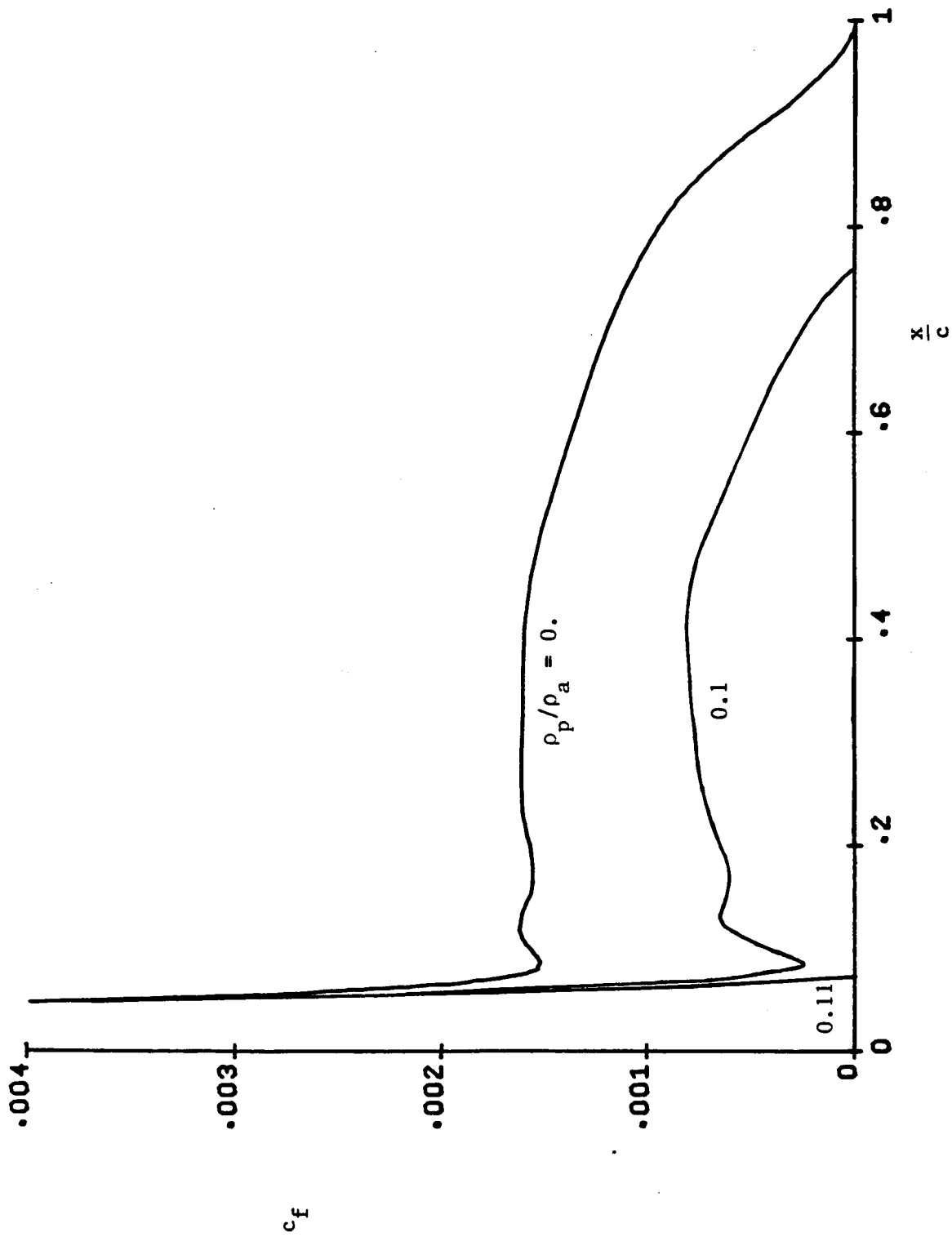


Figure 5.1 Variation of the local coefficient of skin friction as a function of distance from the stagnation point, with rainfall rate (represented by ρ_p) as a parameter, on an NACA 64-210 airfoil at $\alpha = 12^\circ$ for $l_{cm}/c = 0.001$, $v_{pm}/u_\infty = 0.4$, and $Re = 3.5 \times 10^7$.

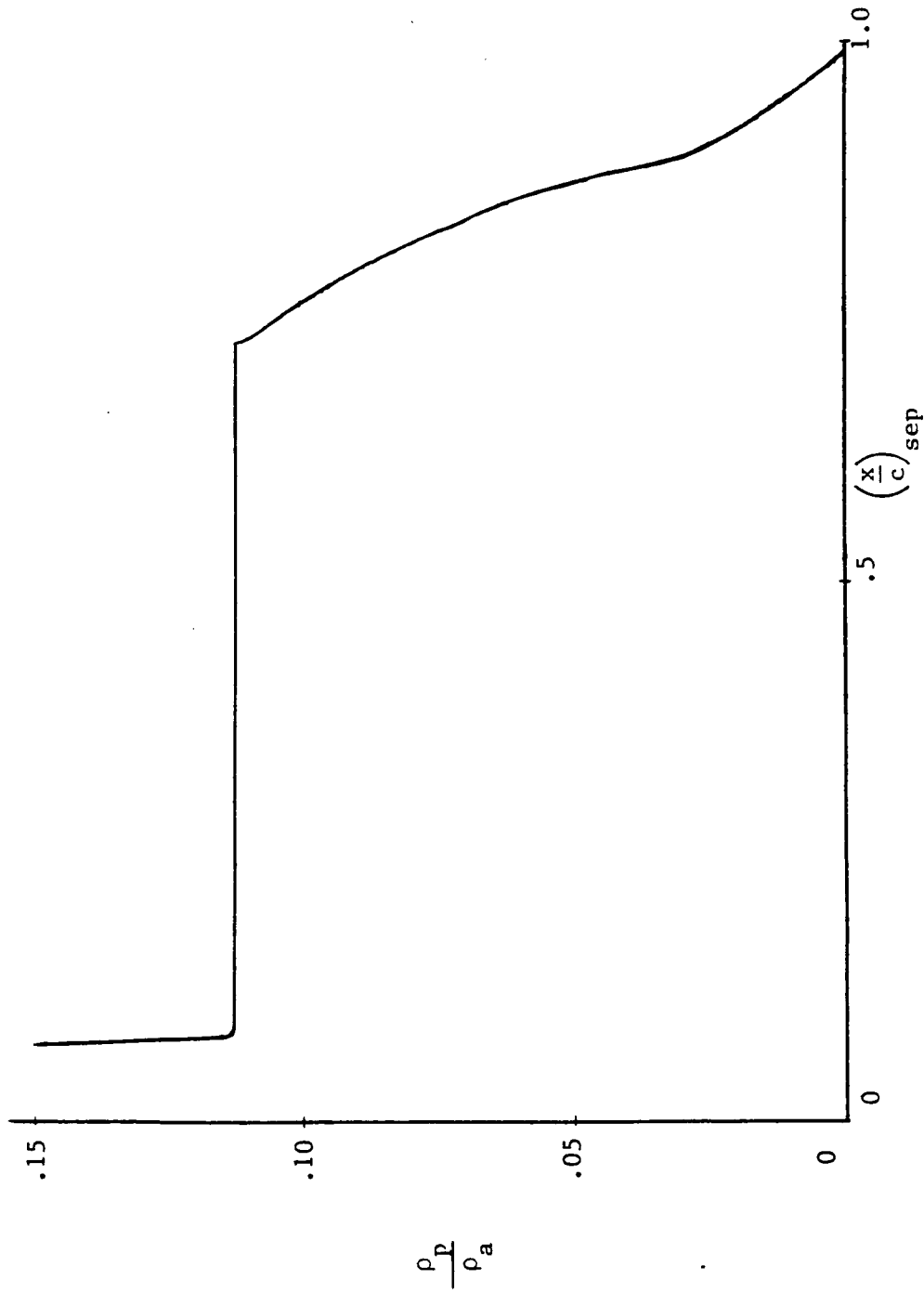


Figure 5.2 Variation of the location of separation as a function of rainfall rate (represented by ρ_p) on an NACA 64-210 airfoil at $\alpha = 12^\circ$ for $l_{cm}/c = 0.001$, $v_{pm}/u_\infty = 0.4$, and $Re = 3.5 \times 10^7$.

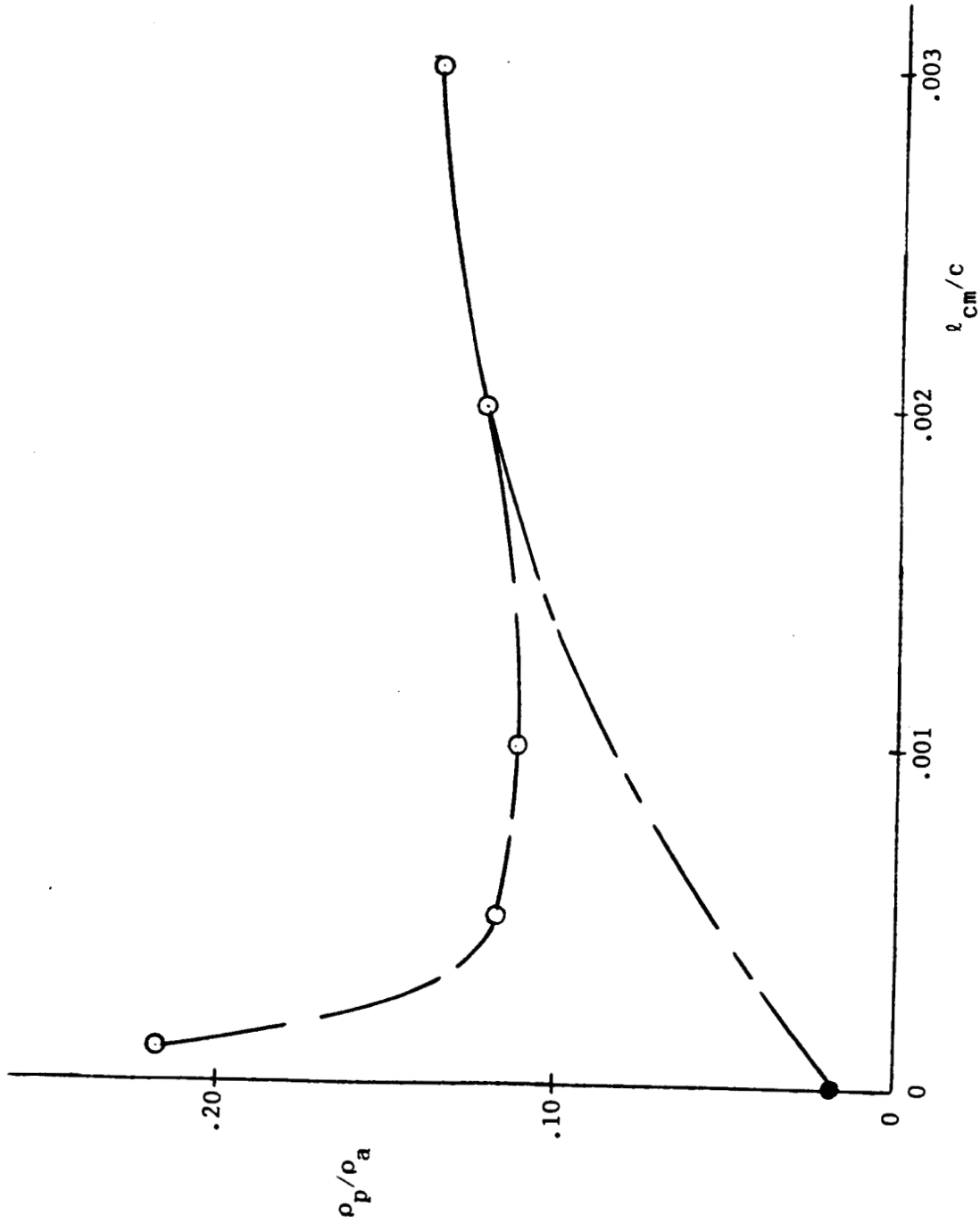


Figure 5.3 Variation of the critical value of ρ_p as a function of l_{cm}/c for an NACA 64-210 airfoil at $\alpha = 12^\circ$ with $v_{pm}/u_\infty = 0.4$ and $Re = 3.5 \times 10^7$.

this phenomenon showed it to be related to the fact that as l_c becomes small compared to the boundary-layer thickness, the effect of the particles on the vertical momentum in the boundary layer needs to be included in the calculations. As mentioned in Section 4.1, this is not possible in the ARB code, but a way was found to get around this problem, and it certainly is a problem, by using the surface gas injection feature of ARB for the limit $l_c = 0$. The result of such a calculation is shown by the filled circle for $l_{cm}/c = 0$. For the purposes of estimation, the authors, for want of any better method, have faired a smooth curve shown by the dot-dash curve in Figure 5.3, between this point and the other points we believe to be valid.

Curves such as that shown in Figure 5.3 have been calculated for a number of Reynolds numbers and two values of the ratio v_{pm}/u_∞ . Summary plots of this nature obtained from many runs are shown in Figures 5.4 and 5.5.

Additional scales have been included on these plots. If equations 13 and 14 of Section 2 are combined, we find

$$N_D = \frac{16}{3f} \frac{c}{l_{cm}}$$

where l_{cm} has been used instead of l_c because the value of V meant in the definition of $N_D (= \rho_a V^2 c / \sigma_w)$ is here taken to be the speed of the aircraft, u_∞ . (See Section 4.2.) Taking the value of f , the portion of the kinetic energy of the drops impinging on the surface converted to surface energy, to be 1/2, we can write

$$N_D \cong \frac{10}{l_{cm}/c}$$

Values of N_D thus calculated are indicated as additional horizontal scales in Figures 5.4 and 5.5. The additional vertical scales are rainfall rates, obtained from ρ_p/ρ_a under the following assumptions. The settling velocity of the raindrops is taken to be about 5 m/sec and it is assumed that half the

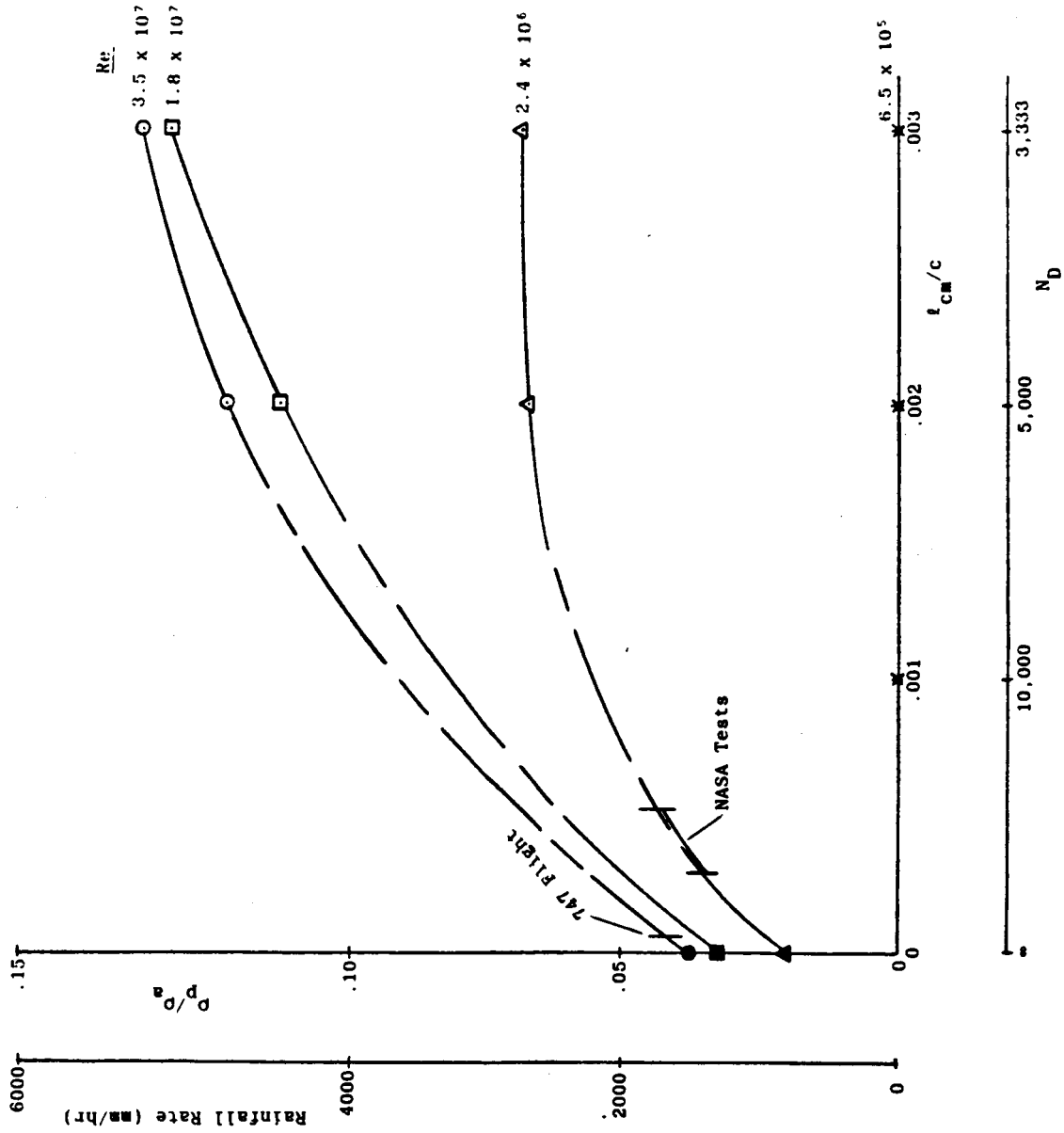


Figure 5.4 Variation of the critical value of p_p or rainfall rate as a function of C_D or N_D , with Reynolds number as a parameter, for an NACA 64-210 airfoil at $\alpha = 12^\circ$ with $v_{pm}/u_\infty = 0.4$.

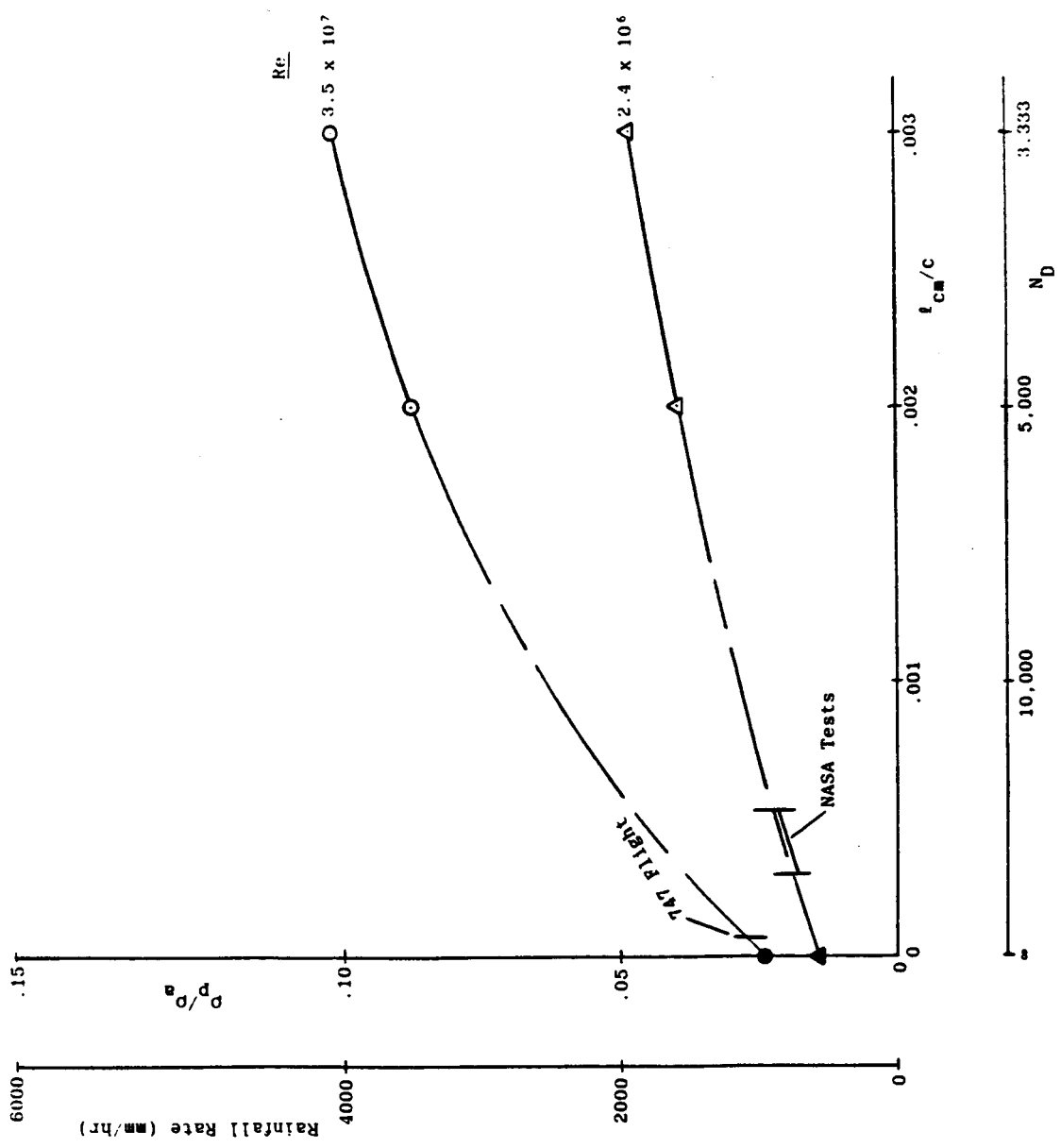


Figure 5.5 Variation of the critical value of ρ_p or rainfall rate as a function of l_{cm}/c or N_D , with Reynolds number as a parameter, for an NACA 64-210 airfoil at $\alpha = 12^\circ$ with $v_{pm}/u_\infty = 0.6$.

water impinging on the wing is splashed back. Then it can be shown that at standard conditions the rainfall rate in mm/hr is approximately $4 \times 10^4 \rho_p / \rho_a$.

Examining Figure 5.4, for $v_{pm}/u_\infty = 0.4$, we note that, as expected, for a low Reynolds number (6.5×10^5) the airfoil stalls even when there is no rainfall. As the Reynolds number is increased to the level of the NASA tests mentioned above (2.4×10^6), the rainfall required to cause early separation decreases as l_{cm}/c decreases, i.e. as N_D increases. For Reynolds numbers typical of transport aircraft (1.8×10^7 and 3.5×10^7) the calculations indicate that the increased Reynolds number offsets the effect of pure size on N_D so that a somewhat larger rainfall rate is required to induce early stall for a 747 aircraft than was found for conditions of the NASA tests. This is an interesting result and is at variance with the pessimistic results of the authors' first extrapolation of the NASA data (see Figure 3.2)

Figure 5.5 shows similar results for $v_{pm}/u_\infty = 0.6$. It was anticipated that this parameter, which relates the normal velocity of the incoming drop to the initial velocity of the droplets resulting from its fracture, would be a very sensitive parameter in the interaction between the droplets and the boundary-layer. A comparison of Figures 5.4 and 5.5 shows this to be the case. For example, the rainfall rate required to induce early separation for the conditions of the NASA tests dropped from about 1400 mm/hr to about 800 mm/hr.

6. Discussion and Recommendations

The computations that have just been presented are believed to give the general trends associated with the phenomenon of premature stall due to coupling of the splash-back droplets with the boundary layer. Clearly the numerical values of rainfall rate to produce premature separation of a given Reynolds number and mixed Weber number (the deposition number N_D) are not exact. However, we believe this to be of the right order of magnitude.

If this conclusion is correct it follows that for rainfall rates approaching 500 mm/hour or greater, commercial aircraft might be subject to rain induced premature stall. The calculations also indicate that both Reynolds number and scale are important in pinning down the values of rainfall rate that will result in early separation due to ejecta coupling with the boundary layer. In view of these facts and in view of the fact that other extremely complex phenomena also have an effect on boundary layer behaviors in the presence of heavy rain, it is clearly necessary to conduct full scale tests if a quantitative assessment of heavy rain hazard is to be made. This is true for simple wings and is certainly even more true of the flapped and slotted wings typical of commercial aircraft.

In regard to analysis, although it is believed that certain trends that have been calculated with the extended ARB program are correct, it has been shown that, if more exact computations are required, a method more powerful than conventional boundary layer theory must be applied. Since such analysis will be expensive, it seems desirable to hold off any further development of analytical capability until such time as both full scale and model tests of the same wing configuration can be completed so that the importance of heavy rain effects on wing performance can be evaluated more precisely.

References

1. Rhode, R. V., "Some Effects of Rainfall on Flight of Airplanes and on Instrument Indications," NACA Tech. Note 803, 1941.
2. Haines, R. A. and Luers, J. K., "Aerodynamic Penalties of Heavy Rain on a Landing Aircraft," J. Aircraft, Vol. 20, No. 2, February 1983.
3. Dunham, E. R., Bezos, G. M., Gentry, C. L. and Melson, E., "Two-Dimensional Wind Tunnel Tests of a Transport-Type Airfoil in a Water Spray," AIAA-85-0258.
4. Donaldson, C. duP., "On the Scaling of the Effect of Heavy Rain on the Maximum Lift of Airfoils, A.R.A.P. Technical Memorandum 85-33, August, 1985.
5. Bilanin, A. J., "Scaling Laws for Testing of High Lift Airfoils Under Heavy Rainfall," presented at AIAA 23rd Aerospace Sciences Mtg., January 1985, Reno, Nevada, AIAA-85-0257.
6. Sullivan, R. D., and Varma, A. K., "ARB: A Program to Compute the Turbulent Boundary Layer on an Arbitrary Body of Revolution," A.R.A.P. Report No. 317, January 1978. Also: Sullivan, R. D., "ARB: A Supplementary Manual," A.R.A.P. Tech Memo 80-16, September 1980.
7. Schlichting, H., **Boundary Layer Theory**, Fourth Edition, McGraw-Hill Book Co., Inc., translated by J. Kestin, 1960.

Standard Bibliographic Page

1. Report No. NASA CR-178248		2. Government Accession No.		3. Recipient's Catalog No.	
4. Title and Subtitle The Effect of Heavy Rain on an Airfoil at High Lift				5. Report Date March 1987	
				6. Performing Organization Code	
7. Author(s) Coleman duP. Donaldson and Roger D. Sullivan				8. Performing Organization Report No. ARAP Report No. 597	
				10. Work Unit No.	
9. Performing Organization Name and Address A.R.A.P. Group Titan Systems, Inc. Princeton, New Jersey 08540				11. Contract or Grant No. NAS1-18088	
				13. Type of Report and Period Covered Contractor Report	
12. Sponsoring Agency Name and Address National Aeronautics and Space Administration Washington, DC 20546				14. Sponsoring Agency Code 505-45-13-01	
15. Supplementary Notes Langley Technical Monitor: R. Earl Dunham, Jr.					
16. Abstract <p>Although the effect of heavy rain on aircraft performance was discussed as early as 1941 by Rhode (1), no serious studies of the relationship of heavy rain to aircraft safety were made until Luers suggested in 1981 that the torrential rain that often occurs at the time of severe wind shear might substantially increase the danger to aircraft operating at slow speeds and high lift in the vicinity of airports. While Luer's ideas were not published until early 1983 (2), appropriate measures were taken by NASA to study the effect of heavy rain on the lift of wings typical of commercial aircraft. These tests, reported by Dunham, Bezos, Gentry, and Melson (3), were the subject of a number of discussions between the senior author of this report and Mr. Earl Dunham of NASA during the fall of 1984. One of the aspects of these tests that seemed confirmed by the data was the existence of a "velocity effect" on the lift data. The data seemed to indicate that when all the normal non-dimensional aerodynamic parameters were used to sort out the data, the effect of velocity was not accounted for, as it usually is, by the effect of dynamic pressure. Indeed, the measured lift coefficients at high lift indicated a drop-off in lift coefficient for the same free-stream water content as velocity was increased.</p>					
17. Key Words (Suggested by Authors(s)) Heavy rain Airfoil Boundary layer High lift			18. Distribution Statement Unclassified - Unlimited Subject Category 02		
19. Security Classif.(of this report) Unclassified		20. Security Classif.(of this page) Unclassified		21. No. of Pages 34	22. Price A03

For sale by the National Technical Information Service, Springfield, Virginia 22161